Characterization and function of medium and large extracellular vesicles from plasma and urine by surface antigens and Annexin V

Ko Igami [1, 2, 3], **Takeshi Uchiumi** [Corresp., 1, 4], **Saori Ueda** [1], **Kazuyuki Kamioka** [2, 5], **Daiki Setoyama** [1], **Kazuhito Gotoh** [1], **Masaru Akimoto** [1], **Shinya Matsumoto** [1], **Dongchon Kang** [1]

[1] Department of Clinical Chemistry and Laboratory Medicine, Kyushu University Graduate School of Medical Sciences, Kyushu University, Fukuoka, Japan
[2] Kyushu Pro Search Limited Liability Partnership, Fukuoka, Japan
[3] Business Management Division, Clinical Laboratory Business Segment, LSI Medience Corporation, Tokyo, Japan
[4] Clinical Chemistry, Division of Biochemical Science and Technology, Department of Health Sciences, Faculty of Medical Sciences,, Kyushu University, Fukuoka, Japan
[5] Department of Medical Solutions, LSI Medience Corporation, Tokyo, Japan

Corresponding Author: Takeshi Uchiumi
Email address: uchiumi@cclm.med.kyushu-u.ac.jp

Background. Extracellular vesicles (EVs) are released by most cell types and are involved in multiple basic biological processes. Medium/large EVs (m/lEVs), which is different size from exosome, plays an important role in the coagulation in blood, and is secreted from cancer cells, etc., suggesting functions related to malignant transformation. The m/lEVs levels in blood or urine may help unravel pathophysiological findings in many diseases. However, it remains unclear how many naturally-occurring m/lEV subtypes exist as well as how their characteristics and functions differ from one another. **Methods**. We used the blood and urinal sample from each 10 healthy donors for analysis. Using a flow cytometer, we focus on characterization of EVs with large sizes (>200nm) that are different from exosomes. We also searched for a membrane protein for characterization with a flow cytometer using shotgun proteomics. Then we identified m/lEVs pelleted from plasma and urine samples by differential centrifugation and characterized by flow cytometry. **Results**. Using proteomic profiling, we identified several proteins involved in m/lEV biogenesis including adhesion molecules, peptidases and exocytosis regulatory proteins. In healthy human plasma, we could distinguish m/lEVs derived from platelets, erythrocytes, monocytes/macrophages, T and B cells, and vascular endothelial cells with more than two positive surface antigens. The ratio of phosphatidylserine appearing on the membrane surface differed depending on the cell-derived m/lEVs. In urine, 50% of m/lEVs were Annexin V negative but contained various membrane peptidases derived from renal tubular villi. Urinary m/lEVs, but not plasma m/lEVs, showed peptidase activity. The knowledge of the new characteristics is considered to be useful as a diagnostic material

and the newly developed method suggests the possibility of clinical application.

Characterization and function of medium and large extracellular vesicles from plasma and urine by surface antigens and Annexin V

Ko Igami[1, 2, 3], Takeshi Uchiumi[1,4]*, Saori Ueda[1], Kazuyuki Kamioka[2, 5], Daiki Setoyama[1], Kazuhito Gotoh[1], Masaru Akimoto[1], Shinya Matsumoto[1] and Dongchon Kang[1]

[1]Department of Clinical Chemistry and Laboratory Medicine, Kyushu University Graduate School of Medical Sciences, 3-1-1, Maidashi, Higashi-ku, Fukuoka 812-8582, Japan.
[2]Kyushu Pro Search Limited Liability Partnership, 4-1, Kyudaishimmachi, Nishi-ku, Fukuoka, 819-0388, Japan.
[3]Business Management Division, Clinical Laboratory Business Segment, LSI Medience Corporation, 13-4, Uchikanda 1-chome, Chiyoda-ku, Tokyo, 101-8517, Japan.
[4]Clinical Chemistry, Division of Biochemical Science and Technology, Department of Health Sciences, Faculty of Medical Sciences, Kyushu University, Fukuoka, Japan
[5] Department of Medical Solutions, LSI Medience Corporation, 3-30-1, Shimura, Itabashi-ku, Tokyo, 174-8555, Japan.

*Correspondence Author:
Takeshi Uchiumi, Department of Clinical Chemistry and Laboratory Medicine, Kyushu University Graduate School of Medical Sciences, 3-1-1, Maidashi, Higashi-ku, Fukuoka 812-8582, Japan.
E-mail: uchiumi@cclm.med.kyushu-u.ac.jp

Abstract

Background. Extracellular vesicles (EVs) are released by most cell types and are involved in multiple basic biological processes. Medium/large EVs (m/lEVs), which is different size from exosome, plays an important role in the coagulation in blood, and is secreted from cancer cells, etc., suggesting functions related to malignant transformation. The m/lEVs levels in blood or urine may help unravel pathophysiological findings in many diseases. However, it remains unclear how many naturally-occurring m/lEV subtypes exist as well as how their characteristics and functions differ from one another.

Methods. We used the blood and urinal sample from each 10 healthy donors for analysis. Using a flow cytometer, we focus on characterization of EVs with large sizes (>200nm) that are different from exosomes. We also searched for a membrane protein for characterization with a flow cytometer using shotgun proteomics. Then we identified m/lEVs pelleted from plasma and urine samples by differential centrifugation and characterized by flow cytometry.

Results. Using proteomic profiling, we identified several proteins involved in m/lEV biogenesis including adhesion molecules, peptidases and exocytosis regulatory proteins. In healthy human plasma, we could distinguish m/lEVs derived from platelets, erythrocytes, monocytes/macrophages, T and B cells, and vascular endothelial cells with more than two positive surface antigens. The ratio of phosphatidylserine appearing on the membrane surface differed depending on the cell-derived m/lEVs. In urine, 50% of m/lEVs were Annexin V negative but contained various membrane peptidases derived from renal tubular villi. Urinary m/lEVs, but not plasma m/lEVs, showed peptidase activity. The knowledge of the new characteristics is considered to be useful as a diagnostic material and the newly developed method suggests the possibility of clinical application.

Introduction

Extracellular vesicles (EVs) play essential roles in cell-cell communication and are diagnostically significant molecules. EVs are secreted from most cell types under normal and pathophysiological conditions (Iraci et al. 2016; Ohno et al. 2013). These membrane vesicles can be detected in many human body fluids and are thought to have signaling functions in interactions between cells. Analysis of EVs may have applications in therapy, prognosis, and biomarker development in various fields. The hope is that using EV analysis, clinicians will be able to detect the presence of disease as well as to classify its progression using noninvasive methods such as liquid biopsy (Boukouris & Mathivanan 2015; Piccin 2014; Piccin et al. 2015a; Piccin et al. 2017a; Piccin et al. 2017b; Piccin et al. 2015b).

Medium/large extracellular vesicles (m/lEVs) can be classified based on their cellular origins, biological functions and biogenesis (El Andaloussi et al. 2013). In a broad sense, they can be classified into m/lEVs with diameters of 100–1000 nm diameter (membrane blebs) and smaller EVs (e.g. exosomes) with diameters of 30–150 nm (Raposo & Stoorvogel 2013; Robbins & Morelli 2014). The m/lEVs are generated by direct outward budding from the plasma membrane (D'Souza-Schorey & Clancy 2012), while smaller EVs (e.g. exosomes) are produced via the endosomal pathway with formation of intraluminal vesicles by inward budding of multivesicular bodies (MVBs) (Raposo & Stoorvogel 2013). In this study, we analyzed the physical characteristics of EVs from 200 nm to 800 nm in diameter which we refer to as m/lEVs as per the MISEV2018 guidelines (Thery et al. 2018).

Recently, the clinical relevance of EVs has attracted significant attention. In particular, m/lEVs play an important role in tumor invasion (Clancy et al. 2015). m/lEVs in blood act as a coagulant factor and have been associated with sickle cell disease, sepsis, thrombotic thrombocytopenic purpura, and other diseases (Piccin et al. 2007; Piccin et al. 2017a; Piccin et al. 2017b). A possible role for urinary m/lEVs in diabetic nephropathy was also reported (Sun et al. 2012). In recent years, the clinical applications of exosomes have been developed (Yoshioka et al. 2014). However, because characterization of exosomes is analytically challenging, determining the cells and tissues from which exosomes are derived can be difficult. m/lEVs are

generated differently from exosomes (Mathivanan et al. 2010) but are similar in size and contain many of the same surface antigens. It is widely hypothesized that complete separation of exosomes and m/lEVs is likely to be a major challenge, and more effective techniques to purify and characterize m/lEVs would be extremely valuable.

In this study, we focused on m/lEVs in plasma and urine, which are representative body fluids in clinical laboratories. We purified for m/lEVs based on differential centrifugation and characterized m/lEVs by flow cytometry and mass spectrometry analysis and described the basic properties (characterizing surface antigen and orientation of phosphatidylserine and activity of the enzymes) of m/lEV subpopulations in blood and urine.

Materials and Methods

Antibodies and other reagents

The following monoclonal antibodies against human surface antigens were used in this study: anti-CD5(clone: L17F12), anti-CD15 (clone: W6D3), anti-CD41(clone: HIP8), anti-CD45(clone: HI30), anti-CD59 (clone: p282), anti-CD61 (clone: VI-PL2), anti-CD105 (clone: 43A3), anti-CD146(clone: P1H12), anti-CD235a (clone: HI264), anti-CD10 (clone: HI10a), anti-CD13 (clone: WM15), anti-CD26 (clone: BA5b), anti-CD227 (MUC1) (clone: 16A). All antibodies were purchased from BioLegend® (San Diego, CA). FITC-conjugated Annexin V was purchased from BD Biosciences (New Jersey, USA). We used the SPHERO™ Nano Fluorescent Particle Size Standard Kit, Yellow (diameters 0.22, 0.45, 0.88 and 1.35 μm) from Spherotech Inc. for size validation. Normal mouse IgG was purchased from Wako Chemicals (Tokyo, Japan). APC-conjugated normal mouse IgG was produced using the Mix-n-Stain™ APC Antibody Labeling kit from Biotium Inc. Dithiothreitol (DTT) was purchased from Wako Chemicals (Tokyo, Japan). We conducted phase transfer surfactant experiments using “MPEX PTS Reagents for MS” purchased from GL Sciences Inc. and “Trypsin, TPCK Treated” purchased from Thermo Fisher Scientific™. Iodoacetamide was purchased from Wako Chemicals (Tokyo, Japan).

Samples

All studies were approved by the Institutional Review Board of the Kyushu University Hospital, Kyushu University (29-340). Blood samples were collected from 20 male and female participants (23–48 years of age) who were apparently healthy. We received the informed consent from all participants of this study. Samples were collected using a 22-gauge butterfly needle and a slow-fill syringe. After discarding the initial 2–3 mL, blood was dispensed into collection tubes containing ethylenediamine tetra acetic acid (EDTA) (1.6 mg/mL blood). Urine was collected from 20 male healthy subjects (23–46 years of age). The first morning void urine was used for the experiments. The urine samples were collected in a sterile container. In particular, we confirmed that sample used for analysis by flow cytometer were derived from

healthy donors by measuring blood count and creatinine in blood and total urine protein (Supplementary Table.S1).

Isolation of plasma m/lEVs

Essentially platelet-free plasma (PFP) was prepared from EDTA-treated blood by double centrifugation at 2,330 ×*g* for 10 min. To assess residual platelets remaining in this sample, we measured platelet number using the ADVIA® 2120i Hematology System (SIEMENS Healthineers, Erlangen Germany). The number of platelets in this sample was below the limit of detection (1×10^3 cells/μL). We used a centrifugation method to obtain m/lEVs. In an effort to ensure our approach could be applied to clinical testing, we chose a simple and easy method for pretreatment. In an ISEV position paper (Mateescu et al. 2017), Thery's group referred to vesicles sedimenting at 100,000 ×*g* as "small EVs" rather than exosomes, those pelleting at intermediate speed (lower than 20,000 ×*g*) as "medium EVs" (including microvesicles and ectosomes) and those pelleting at low speed (e.g., 2000 ×*g*) as "large EVs". Because these definitions are less biologically meaningful but more experimentally tractable than previously-applied exosome/microvesicle definitions, we attempted biological characterization through subsequent shotgun and flow cytometry analysis.

In flow cytometric analysis, the volume of PFP used in each assay was 0.6 mL from each donor. In electron microscopy, the volume of PFP used was 3 mL. Samples were independent and were treated individually prior to each measurement. PFP was centrifuged at 18,900 ×*g* for 30 min in a fixed-angle rotor. The m/lEV pellet obtained after centrifugation was reconstituted by vortex mixing (1–2 min) with an equivalent volume of Dulbecco's phosphate-buffered saline (DPBS), pH 7.4. The solution was centrifuged at 18,900 ×*g* for 30 min again and the supernatant was discarded.

Isolation of urinary m/lEVs

For isolation of urinary m/lEVs, we modified a urinary exosome extraction protocol (Fernandez-Llama et al. 2010). The centrifugation conditions were identical for plasma and urine so that the size and the density of m/lEVs were similar, enabling comparison of plasma and urinary m/lEVs.

In flow cytometric analysis, the volume of urine used for each assay was 1.2 mL from each donor. In electron microscopy, the volume of urine used was 15 mL. Samples were independent and were treated individually prior to each measurement. Collected urine was centrifuged at 2,330 ×*g* for 10 min twice. The supernatant was centrifuged at 18,900 ×*g* for 30 min in a fixed-angle rotor. The m/lEV pellet obtained from centrifugation was reconstituted by vortex mixing (1–2 min) with 0.2 mL of DPBS followed by incubation with DTT (final concentration 10 mg/mL) at 37°C for 10–15 min. The samples were centrifuged again at 18,900 ×*g* for 30 min and the supernatant was discarded. Addition of DTT, a reducing agent, reduced the formation of Tamm-Horsfall protein (THP) polymers. THP monomers were removed from m/lEVs after centrifugation. DTT-containing DPBS solutions were filtered through 0.1-μm filters (Millipore).

Flow cytometric analysis of m/lEVs

After resuspending m/lEV pellets in 60 μL of DPBS, we added saturating concentrations of several labelled antibodies, Annexin V and normal mouse IgG and incubated the tubes in the dark, without stirring, for 15–30 min at room temperature. In one case, we added labelled antibodies directly to 60 μL of PFP for staining. We resuspended stained fractions in Annexin V binding buffer (BD Biosciences: 10 mM HEPES, 0.14 mM NaCl, 2.5 mM $CaCl_2$, pH 7.4) for analysis by flow cytometry. DPBS and Annexin V binding buffer were filtered through 0.1-μm filters (Millipore). Flow cytometry was performed using a FACSVerse™ flow cytometer (BD Biosciences). The flow cytometer was equipped with 405 nm, 488 nm and 638 nm lasers to detect up to 13 fluorescent parameters. The flow rate was 12 μL/min. Forward scatter voltage was set to 381, side scatter voltage was set to 340, and each threshold was set to 200. Details of excitation (Ex.) and emission (Em.) wavelengths as well as voltages described in supplements Fig. Flow cytometry was performed using FACSuite™ software (BD Biosciences) and data were analyzed using FlowJo software. The authors have applied for the following patents for the characterization method of m/lEVs isolated from plasma and urine with a flow cytometer: JP2018-109402(plasma) and JP2018-109403(urine).

Nanoparticle tracking analysis (NTA)

NTA measurements were performed using a NanoSight LM10 (NanoSight, Amesbury, United Kingdom). After resuspending mEV pellets in 50 μL of DPBS, samples were diluted eight-fold (plasma) and 100-fold (urinary) with PBS prior to measurement. Particles in the laser beam undergo Brownian motion and videos of these particle movements are recorded. NTA 2.3 software then analyses the video and determines the particle concentration and the size distribution of the particles. Twenty-five frames per second were recorded for each sample at appropriate dilutions with a "frames processed" setting of 1500. The detection threshold was set at "7 Multi" and at least 1,000 tracks were analyzed for each video.

Electron microscopy

For immobilization, we added 100 μL of PBS and another 100 μL of immobilization solution (4% paraformaldehyde, 4% glutaraldehyde, 0.1 M phosphate buffer, pH 7.4) to m/lEV pellets. After stirring, we incubated at 4°C for 1 h. For negative staining, the samples were adsorbed to formvar film-coated copper grids (400 mesh) and stained with 2% phosphotungstic acid, pH 7.0, for 30 s. For observation and imaging, the grids were observed using a transmission electron microscope (JEM-1400Plus; JEOL Ltd., Tokyo, Japan) at an acceleration voltage of 100 kV. Digital images (3296 × 2472 pixels) were taken with a CCD camera (EM-14830RUBY2; JEOL Ltd., Tokyo, Japan).

Protein digestion

We used approximately 50 mL of pooled healthy plasma and 100 mL of pooled healthy male urine from five healthy subjects for digestion of m/lEVs.

In plasma the following process is the same as "Isolation of plasma m/lEVs" section. We repeated 18,900 ×g centrifugation washing steps three times to reduce levels of contaminating free plasma proteins and small EVs for shotgun analysis. After the last centrifugation, we removed supernatants and froze the samples.

In urine the following process is the same as "Isolation of urinary m/lEVs" section. We repeated washing steps twice (after DTT treatment) to reduce levels of contaminating free urinary proteins and small EVs for shotgun analysis. We removed supernatants and froze the samples.

To discover characterizing surface antigen by flowcytometry, the sample was digested using a phase transfer surfactant-aided procedure so that many hydrophobic membrane proteins could be detected (Chen et al. 2017). The precipitated frozen fractions of plasma and urine were thawed at 37°C, and then m/lEVs were solubilized in 250 µL of lysis buffer containing 12 mM sodium deoxycholate and 12 mM sodium lauroyl sarcosinate in 100 mM Tris·HCl, pH 8.5. After incubating for 5 min at 95°C, the solution was sonicated using an ultrasonic homogenizer. Protein concentrations of the solutions were measured using a bicinchoninic acid assay (Pierce™ BCA Protein Assay Kit; Thermo Fisher Scientific).

Twenty microliters of the dissolved pellet (30 µg protein) were used for protein digestion. Proteins were reduced and alkylated with 1 mM DTT and 5.5 mM iodoacetamide at 25°C for 60 min. Trypsin was added to a final enzyme:protein ratio of 1:100 (wt/wt) for overnight digestion. Digested peptides were acidified with 0.5% trifluoroacetic acid (final concentration) and 100 µL of ethyl acetate was added for each 100 µL of digested m/lEVs. The mixture was shaken for 2 min and then centrifuged at 15,600 ×*g* for 2 min to obtain aqueous and organic phases. The aqueous phase was collected and desalted using a GL-Tip SDB column (GL Sciences Inc).

LC-MS/MS analysis

Digested peptides were dissolved in 40 µL of 0.1% formic acid containing 2% (v/v) acetonitrile and 2 µL were injected into an Easy-nLC 1000 system (Thermo Fisher Scientific). Peptides were separated on an Acclaim PepMap™ RSLC column (15 cm × 50 µm inner diameter) containing C18 resin (2 µm, 100 Å; Thermo Fisher Scientific™), and an Acclaim PepMap™ 100 trap column (2 cm× 75 µm inner diameter) containing C18 resin (3 µm, 100 Å; Thermo Fisher Scientific™). The mobile phase consisted of 0.1% formic acid in ultrapure water (buffer A). The elution buffer was 0.1 % formic acid in acetonitrile (buffer B); a linear 200 min gradient from 0%–40% buffer B was used at a flow rate of 200 nL/min. The Easy-nLC 1000 was coupled via a nanospray Flex ion source (Thermo Fisher Scientific™) to a Q Exactive™ Orbitrap (Thermo Fisher Scientific™). The mass spectrometer was operated in data-dependent mode, in which a full-scan MS (from 350 to 1,400 m/z with a resolution of 70,000, automatic gain control (AGC) 3E+06, maximum injection time 50 ms) was followed by MS/MS on the 20 most intense ions

(AGC 1E+05, maximum injection time 100 ms, 4.0 m/z isolation window, fixed first mass 100 m/z, normalized collision energy 32 eV).

Proteome Data Analysis

Raw MS files were analyzed using Proteome Discoverer software version 1.4 (Thermo Fisher Scientific™) and peptide lists were searched against the Uniprot Proteomes-Homo sapiens FASTA (Last modified November 17, 2018) using the Sequest HT algorithm. Initial precursor mass tolerance was set at 10 ppm and fragment mass tolerance was set at 0.6 Da. Search criteria included static carbamidomethylation of cysteine (+57.0214 Da), dynamic oxidation of methionine (+15.995 Da) and dynamic acetylation (+43.006 Da) of lysine and arginine residues.

Gene ontology analysis and gene enrichment analysis

We conducted GO analysis using DAVID (https://david.ncifcrf.gov) to categorize the proteins identified by shotgun analysis and used Metascape (http://metascape.org/gp/index.html#/main/step1) for gene enrichment analysis. We uploaded the UNIPROT_ACCESSION No. for each protein.

Extracellular vesicle preparation from isolated erythrocytes

Whole blood was collected by the same method as above and centrifuged at 2,330 ×*g* for 10 min. After removal of the buffy coat and supernatant plasma, the remaining erythrocytes were washed three times by centrifugation at 2,330 ×*g* for 10 min and the erythrocyte pellet was resuspended in DPBS. EVs were generated from the washed erythrocytes by stimulation in the presence of 2.5 mM $CaCl_2$ (10 mM HEPES, 0.14 mM NaCl, 2.5 mM $CaCl_2$, pH 7.4) for 1 h at room temperature under rotating conditions. Erythrocytes were removed by centrifugation at 2,330 ×*g* for 10 min and the EV rich supernatant was subsequently centrifuged (18,900 ×*g* for 30 min) to pellet the EVs. EVs were resuspended in DPBS.

Dipeptidyl peptidase IV (DPP4 : CD26) activity assay

DPP4 activity was measured in the plasma and urine of six individuals (different from plasma donors). The method was previously published in part (Kawaguchi et al. 2010). DPP4 activity was measured via the fluorescence intensity of 7-amino-4-methylcoumarin (AMC) after its dissociation from the synthetic substrate (Gly-Pro-AMC • HBr) catalyzed by DPP4.

253 Experiments were performed in 96-well black plates. Titrated AMC was added to each well to
254 prepare a standard curve. Fluorescence intensity was measured after incubating substrate with
255 urine samples for 10 min. The enzyme reaction was terminated by addition of acetic acid. The
256 fluorescence intensity (Ex. = 380 nm and Em. = 460 nm) was measured using Varioskan Flash
257 (Thermo Fisher Scientific™). DPP4 activity assays were performed by Kyushu Pro Search LLP
258 (Fukuoka, Japan).

Results

Isolation and characterization of m/lEVs from plasma and urine.

The workflow for the isolation and enrichment of m/lEVs for proteomic and flow cytometric analyses is illustrated in Fig.1A and 1B. m/lEVs from human plasma samples were isolated by high-speed centrifugation, an approach used in previous studies (Jayachandran et al. 2012). For isolation of m/lEVs from urine, DTT, a reducing agent, was used to remove THP polymers because these non-specifically interact with IgGs.

Transmission electron microscopy revealed that almost all m/lEVs were small, closed vesicles with a size of approximately 200 nm that were surrounded by lipid bilayer (Fig. 1C–H). In plasma, we observed EVs whose membranes were not stained either inside or on the surface (Fig. 1C, 1D); we also observed EVs whose forms were slightly distorted (Fig. 1E). In urine, a group of EVs with uneven morphology and EVs with interior structures were observed (Fig. 1F–1H). Apoptotic bodies, cellular debris, and protein aggregates were not detected.

No EVs with diameters greater than 800 nm were observed by NTA (Supplementary Fig.S1) and flow cytometry can detect only EVs with diameters larger than 200 nm. Together, these data suggested that we characterized m/lEVs between 200 nm and 800 nm in diameter from plasma and urine by flow cytometry analysis.

Side-scatter events from size calibration beads of (diameters: 0.22, 0.45, 0.88 and 1.35 μm) were resolved from instrument noise using a FACS Verse flow cytometer (Supplementary Fig.S2A). Inspection of the side-scatter plot indicated that 0.22 μm was the lower limit for bead detection. More than 90% of m/lEVs isolated from plasma and urine showed side-scatter intensities lower than those of 0.88-μm calibration beads (Fig. 2A–D). m/lEVs were heterogeneous in size, with diameters ranging from 200–800 nm in plasma and urine (Fig. 2A–D). Fluorescently-labeled mouse IgG was used to exclude nonspecific IgG-binding fractions (Supplementary Fig.S2 B and C). In this experiment, we characterized m/lEVs with diameters ranging from 200–800 nm. NTA analysis shows less than 100nm size particles in the plasma fraction extracted by centrifugation, but we focused on particles over 200nm using a flow

cytometer. Using these methods, we observed an average of 8×10^5 and 1×10^5m/lEVs in each mL of plasma and urine by flow cytometry observation.

Shotgun proteomic analysis of plasma and urine EVs.

To analyze the protein components and discover characterizing surface antigen of m/lEVs present in plasma and urine of five healthy individuals, we performed LC-MS/MS proteomic analysis. A total of 593 and 1,793 proteins were identified in m/lEVs from plasma and urine, respectively (Fig. 3A and Supplementary Table S2 and Table S3). Scoring counts using the SequestHT algorithm for the top 20 most abundant proteins are shown in Table 1 and 2. We detected cytoskeleton-related protein such as actin, ficolin-3 and filamin and cell-surface antigen such as CD5, band3 and CD41 in plasma. We also identified actin filament-related proteins such as ezrin, radixin, ankylin and moesin which play key roles in cell surface adhesion, migration and organization in both plasma and urine. In urine, several types of peptidases (membrane alanine aminopeptidase or CD13; neprilysin or CD10; DPP4 or CD26) and MUC1 (mucin 1 or CD227) were detected in high abundance, and these proteins were used to characterize m/lEVs by flow cytometric analysis (Table 2 and Supplementary Table S3). We demonstrated that the isolated m/lEVs showed high expression of tubulin and actinin, while the tetraspanins CD9 and CD81 that are often used as exosome markers were only weakly identified. These data suggest that m/lEVs differ from small EVs including exosomes (Supplementary Table S4).

As shown in Fig. 3A and Supplementary Fig S3, about 10% of urinary EVs proteins were also identified in plasma EVs. Urinary EVs in the presence of blood contaminants were also observed in previous studies (Smalley et al. 2008). These result suggest that m/lEVs in plasma were excreted in the urine via renal filtration and not reabsorbed. Gene ontology analysis of the identified proteins indicated overall similar cellular components in plasma and urine m/lEVs (Fig. 3B). The results of gene set enrichment analysis by metascape are shown for plasma and urine m/lEVs (Fig. 3C, D and Supplementary Table S5 and Table S6). The most commonly-observed functions in both plasma and urine were "regulated exocytosis", "hemostasis" and "vesicle-mediated transport". In plasma, several functions of blood cells were observed, including "complement and coagulation cascades" and "immune response". Moreover, analysis

of urinary EVs showed several characteristic functions including "transport of small molecules", "metabolic process" and "cell projection assembly". This may reflect the nature of the kidney, the urinary system and tubular villi. These data demonstrate the power of data-driven biological analyses.

Characterization of plasma EVs by flow cytometry.

Next, we characterized m/lEVs in plasma by flow cytometry using antibodies against several surface antigens and Annexin V. To eliminate nonspecific adsorption, we excluded the mouse IgG-positive fraction. (Supplementary Fig.S2B) Eliminating non-specific reactions to antibodies is important in using human body fluids as diagnostic materials for immunological measurements. By adding mouse IgG-APC to the system, we observed accurate flow cytometry image in which specific surface antigens were recognized by following two points: 1) blocking of non-specific reaction sites, 2) gate-out of positive non-specific reaction. We characterized positive m/lEVs using surface antigens detected by shotgun proteomic analysis and Annexin V (Fig. 4A–L).

To characterize m/lEVs derived from erythrocytes, T and B cells, macrophages/monocytes, granulocytes, platelets and endothelial cells, we selected nine antigens described in Fig. 4A. Two or more antigens were used for characterization of m/lEVs: for example, CD59 and CD235a double-positive and CD45-negative m/lEVs were classified as erythrocyte-derived m/lEVs (Supplementary Fig. S4B). We confirmed that m/lEVs isolated from erythrocytes in vitro and erythrocytes derived m/lEVs from plasma are characterized by CD59 and CD235a double-positive and CD45-negative (Supplementary Fig. S5). Determined positive area by addition of EDTA (Supplementary Fig. S2D), we also show Annexin V staining for the m/lEVs corresponding to these five classifications (Fig. 4B–L). We integrated these characterizations and assessed the distribution of EV classifications among ten healthy subjects (Fig. 4M). The results suggested that no major differences in the ratios of fractions in these ten subjects and thus these definitions may be used for pathological analysis.

We found that 10% and 35% of m/lEVs were derived from erythrocytes and platelets, respectively. However, only 0.5%, 0.6% and 0.1% of m/lEVs were derived from macrophages,

leukocytes and endothelial cells, respectively suggesting that the ratio of m/lEVs of different cellular origins is dependent on the number of cells present in plasma (Fig. 4M). We also observed that most m/lEVs derived from erythrocytes and macrophages were Annexin V positive (Fig. 4 N and O). By contrast, many Annexin V negative m/lEVs were identified among platelet- and T and B cell-derived m/lEVs (Fig. 4 P and Q). Especially about erythrocyte-derived m/lEVs other studies have shown high percentages of phosphatidylserine-positive(:Annexin V positive) m/lEVs after red blood cell storage under blood bank conditions that these results are consistent (Gao et al. 2013)(Xiong et al. 2011).

In general, it is known that microparicle in blood are known to be exposed to PS on the surface, which is verified by being positive by Annexin5 staining. We found that the degree of exposure of phosphatidylserine to the membrane surface was vary depending on the cell derived from annexin V staining. Thus, the characteristics of m/lEVs can be determined in detail by using AnnexinV and antigenicity. These results suggested that the degree of exposing PS are cell-type specific and that release mechanisms may differ among cell types.

Characterization of urinary EVs by flow cytometry and enzyme activity assay.

In urine, we first removed aggregated m/lEVs and residual THP polymers using labelled normal mouse IgG (Supplementary Fig.S2C). By removing the THP polymer by DTT treatment, many immunological non-specific reactions in flow cytometry observation were eliminated, and the remaining non-specific reactions were completely excluded from the observed image by mouse IgG-positive gating-out (Supplementary Fig.S2F). To characterize urinary m/lEVs, we used surface antigens detected by shotgun proteomic analysis including CD10 (neprilysin), CD13 (alanine aminopeptidase), CD26 (DPP4) and CD227 (MUC1) (Fig. 5A–F). Many m/lEVs in the observation area were triple-positive for CD10, CD13 and CD26, but negative for Annexin V (Fig. 5B–D, Supplementary Fig. S6). Furthermore, MUC1-positive EVs were both Annexin V positive and negative in roughly equivalent frequencies (Fig. 5B, E and F). These results suggested that m/lEVs containing peptidases were released by outward budding directly from the cilial membrane of renal proximal tubule epithelial cells. The results of integrating these characterizations and the distribution of EV classifications among ten healthy subjects are shown

(Fig. 5G–I). These data indicated no major differences in the ratio among these populations, suggesting that our methodology was reliable for m/lEV analysis.

We next verified the CD26 peptidase enzyme activities of m/lEVs in plasma and urine from six individuals. We prepared three fractions: (i) “whole,” in which debris were removed after low speed centrifugation, (ii) “m/lEVs” and (iii) “free (supernatant)” both of which were obtained via high speed centrifugation (18,900 ×*g* for 30 min) (Fig. 5J). We found that more than 20% of DPP4 activity in whole urine was contributed by the EV fraction (Fig. 5K and Supplementary Fig. S7). By contrast, there was no peptidase activity associated with plasma m/lEVs (Fig. 5L). These results suggested that functional CD26 peptidase activity is present in m/lEVs in urine, which may be useful for pathological analysis.

Discussion

In this study, we analyzed m/lEVs using various analytic techniques and found the following four major results. First, it was possible to characterize m/lEVs using multiple surface markers. Second, m/lEVs bear functional enzymes with demonstrable enzyme activity on the vesicle surface. Trird, there are probability of differences in asymmetry of membrane lipids by derived cells. Finally, there was little variation m/lEVs in the plasma and urine of healthy individuals, indicating that our method is useful for identifying cell-derived m/lEVs in these body fluids.

We isolated m/lEVs from plasma and urine that were primarily 200–800 nm in diameter as shown by transmission electron microscopy. A large proportion of proteins detected in m/lEVs using shotgun proteomic analysis were categorized as plasma membrane proteins. Isolation of m/lEVs by centrifugation is a classical technique, but in the present study we further separated and classified the m/lEVs according to their cell types of origin by flow cytometry. The results indicated the validity of the differential centrifugation method (Biro et al. 2003; Piccin et al. 2015a).

Pang et al. (Pang et al. 2018) reported that integrin outside-in signaling is an important mechanism for microvesicle formation, in which the procoagulant phospholipid phosphatidylserine (PS) is efficiently externalized to release PS-exposed microvesicles (MVs). These platelet-derived Annexin V positive MVs were induced by application of a pulling force via an integrin ligand such as shear stress. This exposure of PS allows binding of important coagulation factors, enhancing the catalytic efficiencies of coagulation enzymes. We observed that 50% of m/lEVs derived from leukocytes and platelets were Annexin V positive, suggesting that release PS-positive m/lEVs during activation, inflammation, and injury. It would be interesting to further investigate whether the ratio of Annexin V positive m/lEVs from platelets or leukocytes was an important diagnostic factor for inflammatory disease or tissue injury.

In urinary m/lEVs, we identified aminopeptidases such as CD10, CD13 and CD26 which are localized in proximal renal tubular epithelial cells. The functions of these proteins relating to exocytosis were categorized by gene enrichment analysis. The cilium in the kidney is

409 the site at which a variety of membrane receptors, enzymes and signal transduction molecules
410 critical to many cellular processes function. In recent years, ciliary ectosomes – bioactive
411 vesicles released from the surface of the cilium – have attracted attention (Nager et al. 2017;
412 Phua et al. 2017; Wood & Rosenbaum 2015). We also identified ciliary ectosome formation
413 ESCRT complexes proteins (CHAMP; Supplementary Table S3 and 4) in proteomic analyses,
414 suggesting that our isolation method was valid and the possibility that these proteins were
415 biomarkers of kidney disease. Because triple peptidase positive m/lEVs were negative for
416 Annexin V, the mechanism of budding from cells may not be dependent on scramblase. (Wood
417 & Rosenbaum 2015)

418 Platelet-derived m/lEVs are the most abundant population of extracellular vesicles in
419 blood, and their presence (Piccin et al. 2007) and connection with tumor formation were reported
420 in a recent study (Zmigrodzka et al. 2016). In our study, platelet-derived EVs were observed in
421 healthy subjects and had the highest abundance of Annexin V-positive EVs. In plasma,
422 leukocyte-derived EVs were defined as CD11b/CD66b- or CD15-positive (Sarlon-Bartoli et al.
423 2013). We characterized macrophage/monocyte/granulocyte- and T/B cell-derived EVs based on
424 two specific CD antigens, and we confirmed that EVs derived from these cells were very rare.
425 Importantly, there was little variation in the cellular origins of m/lEVs in samples from ten
426 healthy individuals, indicating that this method was useful for identifying cell-derived m/lEVs.
427 We plan to examine m/lEVs differences in patients with these diseases in the near future.
428 Erythrocyte-derived EVs were also characterized by their expression of CD235a and glycophorin
429 A by flow cytometry (Ferru et al. 2014; Zecher et al. 2014).

430 We also characterized m/lEVs in urine. In kidneys and particularly in the renal tubule,
431 CD10, CD13, CD26 can be detected in high abundance by immunohistochemical staining
432 (website: The Human Protein Atlas). CD10/CD13-double positive labeling can be used for
433 isolation and characterization of primary proximal tubular epithelial cells from human kidney
434 (Van der Hauwaert et al. 2013). DPP4 (CD26) is a potential biomarker in urine for diabetic
435 kidney disease and the presence of urinary m/lEV-bound DPP4 has been demonstrated (Sun et
436 al. 2012). The presence of peptidases on the m/lEV surface, and their major contribution to

peptidase activity in whole urine (Sun et al. 2012), may suggest a functional contribution to reabsorption in the proximal tubules. These observations suggested that the ratio of DPP activity between m/lEVs and total urine can be an important factor in the diagnosis of kidney disease.

MUC1 can also be detected in kidney and urinary bladder by immunohistochemical staining (website: The Human Protein Atlas). Significant increases of MUC1 expression in cancerous tissue and in the intermediate zone compared with normal renal tissue distant from the tumor was observed (Borzym-Kluczyk et al. 2015). In any case, MUC1-positive EVs are thought to be more likely to be derived from the tubular epithelium or the urothelium.

Conclusions

Use of EVs as diagnostic reagents with superior disease and organ specificity for liquid biopsy samples is a possibility. This protocol will allow further study and in depth characterization of EV profiles in large patient groups for clinical applications. We are going to attempt to identify novel biomarkers by comparing healthy subjects and patients with various diseases.

ACKNOWLEDGEMENTS

We thank lab members for reagents, discussions, and critical reading of the manuscript. We are grateful to LSI Medience Corporation for generous support during this study. This work was supported by a Grant-in-Aid for Scientific Research from the Japan Society for the Promotion of Science (JSPS; grant numbers #25253041, #17H01550 and 15H04764) and research funding from LSI Medience Corporation. We thank Edanz Group (www.edanzediting.com/ac) for editing a draft of this manuscript.

Author Contributions

K.I. and T.U. designed the research and wrote the manuscript. S.U., K.G., S.M. and M.A carried out the experiments, obtained reagents and materials, and conducted data analysis. D.S. and N.A.

464 contributed to network analysis. D.K, K.K. and T.U. contributed to flavonoid identification. All
465 authors read and approved the final manuscript.
466
467 **Competing Interests**
468 The authors have read the journal's policy and would like to declare the following competing
469 interests: K.I. is a full-time employee of LSI Medience Corporation. K.K. is a full-time employee
470 of LSI Medience Corporation. K.I. is also seconded to Kyushu Pro Search Limited Liability
471 Partnership from LSI Medience Corporation. K.K. also serves as Kyushu Pro Search Limited
472 Liability Partnership and LSI Medience Corporation and is the representative officer of Kyushu
473 Pro Search Limited Liability Partnership.
474
475
476

Reference

Biro E, Sturk-Maquelin KN, Vogel GM, Meuleman DG, Smit MJ, Hack CE, Sturk A, and Nieuwland R. 2003. Human cell-derived microparticles promote thrombus formation in vivo in a tissue factor-dependent manner. *J Thromb Haemost* 1:2561-2568.

Borzym-Kluczyk M, Radziejewska I, and Cechowska-Pasko M. 2015. Increased expression of MUC1 and sialyl Lewis antigens in different areas of clear renal cell carcinoma. *Clin Exp Nephrol* 19:732-737. 10.1007/s10157-014-1013-y

Boukouris S, and Mathivanan S. 2015. Exosomes in bodily fluids are a highly stable resource of disease biomarkers. *Proteomics Clin Appl* 9:358-367. 10.1002/prca.201400114

Chen IH, Xue L, Hsu CC, Paez JS, Pan L, Andaluz H, Wendt MK, Iliuk AB, Zhu JK, and Tao WA. 2017. Phosphoproteins in extracellular vesicles as candidate markers for breast cancer. *Proc Natl Acad Sci U S A* 114:3175-3180. 10.1073/pnas.1618088114

Clancy JW, Sedgwick A, Rosse C, Muralidharan-Chari V, Raposo G, Method M, Chavrier P, and D'Souza-Schorey C. 2015. Regulated delivery of molecular cargo to invasive tumour-derived microvesicles. *Nat Commun* 6:6919. 10.1038/ncomms7919

D'Souza-Schorey C, and Clancy JW. 2012. Tumor-derived microvesicles: shedding light on novel microenvironment modulators and prospective cancer biomarkers. *Genes Dev* 26:1287-1299. 10.1101/gad.192351.112

El Andaloussi S, Lakhal S, Mager I, and Wood MJ. 2013. Exosomes for targeted siRNA delivery across biological barriers. *Adv Drug Deliv Rev* 65:391-397. 10.1016/j.addr.2012.08.008

Fernandez-Llama P, Khositseth S, Gonzales PA, Star RA, Pisitkun T, and Knepper MA. 2010. Tamm-Horsfall protein and urinary exosome isolation. *Kidney Int* 77:736-742. 10.1038/ki.2009.550

Ferru E, Pantaleo A, Carta F, Mannu F, Khadjavi A, Gallo V, Ronzoni L, Graziadei G, Cappellini MD, and Turrini F. 2014. Thalassemic erythrocytes release microparticles loaded with hemichromes by redox activation of p72Syk kinase. *Haematologica* 99:570-578. 10.3324/haematol.2013.084533

Gao Y, Lv L, Liu S, Ma G, and Su Y. 2013. Elevated levels of thrombin‐generating microparticles in stored red blood cells. *Vox sanguinis* 105:11-17.

Iraci N, Leonardi T, Gessler F, Vega B, and Pluchino S. 2016. Focus on Extracellular Vesicles: Physiological Role and Signalling Properties of Extracellular Membrane Vesicles. *Int J Mol Sci* 17:171. 10.3390/ijms17020171

Jayachandran M, Miller VM, Heit JA, and Owen WG. 2012. Methodology for isolation, identification and characterization of microvesicles in peripheral blood. *J Immunol Methods* 375:207-214. 10.1016/j.jim.2011.10.012

Kawaguchi M, Okabe T, Terai T, Hanaoka K, Kojima H, Minegishi I, and Nagano T. 2010. A time-resolved fluorescence probe for dipeptidyl peptidase 4 and its application in inhibitor screening. *Chemistry* 16:13479-13486. 10.1002/chem.201001077

Mateescu B, Kowal EJ, van Balkom BW, Bartel S, Bhattacharyya SN, Buzas EI, Buck AH, de Candia P, Chow FW, Das S, Driedonks TA, Fernandez-Messina L, Haderk F, Hill AF, Jones JC, Van Keuren-Jensen KR, Lai CP, Lasser C, Liegro ID, Lunavat TR, Lorenowicz MJ, Maas SL, Mager I, Mittelbrunn M, Momma S, Mukherjee K, Nawaz M, Pegtel DM, Pfaffl MW, Schiffelers RM, Tahara H, Thery C, Tosar JP, Wauben MH, Witwer KW, and Nolte-'t Hoen EN. 2017. Obstacles and opportunities in the functional analysis of extracellular vesicle RNA - an ISEV position paper. *J Extracell Vesicles* 6:1286095. 10.1080/20013078.2017.1286095

Mathivanan S, Ji H, and Simpson RJ. 2010. Exosomes: extracellular organelles important in intercellular communication. *J Proteomics* 73:1907-1920. 10.1016/j.jprot.2010.06.006

Nager AR, Goldstein JS, Herranz-Perez V, Portran D, Ye F, Garcia-Verdugo JM, and Nachury MV. 2017. An Actin Network Dispatches Ciliary GPCRs into Extracellular Vesicles to Modulate Signaling. *Cell* 168:252-263 e214. 10.1016/j.cell.2016.11.036

Ohno S, Ishikawa A, and Kuroda M. 2013. Roles of exosomes and microvesicles in disease pathogenesis. *Adv Drug Deliv Rev* 65:398-401. 10.1016/j.addr.2012.07.019

Pang A, Cui Y, Chen Y, Cheng N, Delaney MK, Gu M, Stojanovic-Terpo A, Zhu C, and Du X. 2018. Shear-induced integrin signaling in platelet phosphatidylserine exposure, microvesicle release, and coagulation. *Blood* 132:533-543. 10.1182/blood-2017-05-785253

Phua SC, Chiba S, Suzuki M, Su E, Roberson EC, Pusapati GV, Setou M, Rohatgi R, Reiter JF, Ikegami K, and Inoue T. 2017. Dynamic Remodeling of Membrane Composition Drives Cell Cycle through Primary Cilia Excision. *Cell* 168:264-279 e215. 10.1016/j.cell.2016.12.032

Piccin A. 2014. Endothelial Microparticles and Endothelial Damage:‘The Tip and the Iceberg'. *Acta haematologica* 132:199-199.

Piccin A, Murphy C, Eakins E, Kunde J, Corvetta D, Di Pierro A, Negri G, Guido M, Sainati L, Mc Mahon C, Smith OP, and Murphy W. 2015a. Circulating microparticles, protein C, free protein S and endothelial vascular markers in children with sickle cell anaemia. *J Extracell Vesicles* 4:28414. 10.3402/jev.v4.28414

Piccin A, Murphy WG, and Smith OP. 2007. Circulating microparticles: pathophysiology and clinical implications. *Blood Rev* 21:157-171. 10.1016/j.blre.2006.09.001

Piccin A, Sartori MT, Bisogno G, Van Schilfgaarde M, Saggiorato G, Pierro AM, Corvetta D, Marcheselli L, Andrea M, and Gastl G. 2017a. New insights into sinusoidal obstruction syndrome. *Internal medicine journal* 47:1173-1183.

544 Piccin A, Steurer M, Feistritzer C, Murphy C, Eakins E, Van Schilfgaarde M, Corvetta D, Di Pierro AM,
545 Pusceddu I, and Marcheselli L. 2017b. Observational retrospective study of vascular modulator
546 changes during treatment in essential thrombocythemia. *Translational Research* 184:21-34.
547 Piccin A, Van Schilfgaarde M, and Smith O. 2015b. The importance of studying red blood cells
548 microparticles. *Blood Transfusion* 13:172.
549 Raposo G, and Stoorvogel W. 2013. Extracellular vesicles: exosomes, microvesicles, and friends. *J Cell*
550 *Biol* 200:373-383. 10.1083/jcb.201211138
551 Robbins PD, and Morelli AE. 2014. Regulation of immune responses by extracellular vesicles. *Nat Rev*
552 *Immunol* 14:195-208. 10.1038/nri3622
553 Sarlon-Bartoli G, Bennis Y, Lacroix R, Piercecchi-Marti MD, Bartoli MA, Arnaud L, Mancini J, Boudes
554 A, Sarlon E, Thevenin B, Leroyer AS, Squarcioni C, Magnan PE, Dignat-George F, and Sabatier
555 F. 2013. Plasmatic level of leukocyte-derived microparticles is associated with unstable plaque in
556 asymptomatic patients with high-grade carotid stenosis. *J Am Coll Cardiol* 62:1436-1441.
557 10.1016/j.jacc.2013.03.078
558 Smalley DM, Sheman NE, Nelson K, and Theodorescu D. 2008. Isolation and identification of potential
559 urinary microparticle biomarkers of bladder cancer. *J Proteome Res* 7:2088-2096.
560 10.1021/pr700775x
561 Sun AL, Deng JT, Guan GJ, Chen SH, Liu YT, Cheng J, Li ZW, Zhuang XH, Sun FD, and Deng HP. 2012.
562 Dipeptidyl peptidase-IV is a potential molecular biomarker in diabetic kidney disease. *Diab Vasc*
563 *Dis Res* 9:301-308. 10.1177/1479164111434318
564 Thery C, Witwer KW, Aikawa E, Alcaraz MJ, Anderson JD, Andriantsitohaina R, Antoniou A, Arab T,
565 Archer F, Atkin-Smith GK, Ayre DC, Bach JM, Bachurski D, Baharvand H, Balaj L, Baldacchino
566 S, Bauer NN, Baxter AA, Bebawy M, Beckham C, Bedina Zavec A, Benmoussa A, Berardi AC,
567 Bergese P, Bielska E, Blenkiron C, Bobis-Wozowicz S, Boilard E, Boireau W, Bongiovanni A,
568 Borras FE, Bosch S, Boulanger CM, Breakefield X, Breglio AM, Brennan MA, Brigstock DR,
569 Brisson A, Broekman ML, Bromberg JF, Bryl-Gorecka P, Buch S, Buck AH, Burger D, Busatto S,
570 Buschmann D, Bussolati B, Buzas EI, Byrd JB, Camussi G, Carter DR, Caruso S, Chamley LW,
571 Chang YT, Chen C, Chen S, Cheng L, Chin AR, Clayton A, Clerici SP, Cocks A, Cocucci E, Coffey
572 RJ, Cordeiro-da-Silva A, Couch Y, Coumans FA, Coyle B, Crescitelli R, Criado MF, D'Souza-
573 Schorey C, Das S, Datta Chaudhuri A, de Candia P, De Santana EF, De Wever O, Del Portillo HA,
574 Demaret T, Deville S, Devitt A, Dhondt B, Di Vizio D, Dieterich LC, Dolo V, Dominguez Rubio
575 AP, Dominici M, Dourado MR, Driedonks TA, Duarte FV, Duncan HM, Eichenberger RM,
576 Ekstrom K, El Andaloussi S, Elie-Caille C, Erdbrugger U, Falcon-Perez JM, Fatima F, Fish JE,
577 Flores-Bellver M, Forsonits A, Frelet-Barrand A, Fricke F, Fuhrmann G, Gabrielsson S, Gamez-
578 Valero A, Gardiner C, Gartner K, Gaudin R, Gho YS, Giebel B, Gilbert C, Gimona M, Giusti I,
579 Goberdhan DC, Gorgens A, Gorski SM, Greening DW, Gross JC, Gualerzi A, Gupta GN,

Gustafson D, Handberg A, Haraszti RA, Harrison P, Hegyesi H, Hendrix A, Hill AF, Hochberg FH, Hoffmann KF, Holder B, Holthofer H, Hosseinkhani B, Hu G, Huang Y, Huber V, Hunt S, Ibrahim AG, Ikezu T, Inal JM, Isin M, Ivanova A, Jackson HK, Jacobsen S, Jay SM, Jayachandran M, Jenster G, Jiang L, Johnson SM, Jones JC, Jong A, Jovanovic-Talisman T, Jung S, Kalluri R, Kano SI, Kaur S, Kawamura Y, Keller ET, Khamari D, Khomyakova E, Khvorova A, Kierulf P, Kim KP, Kislinger T, Klingeborn M, Klinke DJ, 2nd, Kornek M, Kosanovic MM, Kovacs AF, Kramer-Albers EM, Krasemann S, Krause M, Kurochkin IV, Kusuma GD, Kuypers S, Laitinen S, Langevin SM, Languino LR, Lannigan J, Lasser C, Laurent LC, Lavieu G, Lazaro-Ibanez E, Le Lay S, Lee MS, Lee YXF, Lemos DS, Lenassi M, Leszczynska A, Li IT, Liao K, Libregts SF, Ligeti E, Lim R, Lim SK, Line A, Linnemannstons K, Llorente A, Lombard CA, Lorenowicz MJ, Lorincz AM, Lotvall J, Lovett J, Lowry MC, Loyer X, Lu Q, Lukomska B, Lunavat TR, Maas SL, Malhi H, Marcilla A, Mariani J, Mariscal J, Martens-Uzunova ES, Martin-Jaular L, Martinez MC, Martins VR, Mathieu M, Mathivanan S, Maugeri M, McGinnis LK, McVey MJ, Meckes DG, Jr., Meehan KL, Mertens I, Minciacchi VR, Moller A, Moller Jorgensen M, Morales-Kastresana A, Morhayim J, Mullier F, Muraca M, Musante L, Mussack V, Muth DC, Myburgh KH, Najrana T, Nawaz M, Nazarenko I, Nejsum P, Neri C, Neri T, Nieuwland R, Nimrichter L, Nolan JP, Nolte-'t Hoen EN, Noren Hooten N, O'Driscoll L, O'Grady T, O'Loghlen A, Ochiya T, Olivier M, Ortiz A, Ortiz LA, Osteikoetxea X, Ostergaard O, Ostrowski M, Park J, Pegtel DM, Peinado H, Perut F, Pfaffl MW, Phinney DG, Pieters BC, Pink RC, Pisetsky DS, Pogge von Strandmann E, Polakovicova I, Poon IK, Powell BH, Prada I, Pulliam L, Quesenberry P, Radeghieri A, Raffai RL, Raimondo S, Rak J, Ramirez MI, Raposo G, Rayyan MS, Regev-Rudzki N, Ricklefs FL, Robbins PD, Roberts DD, Rodrigues SC, Rohde E, Rome S, Rouschop KM, Rughetti A, Russell AE, Saa P, Sahoo S, Salas-Huenuleo E, Sanchez C, Saugstad JA, Saul MJ, Schiffelers RM, Schneider R, Schoyen TH, Scott A, Shahaj E, Sharma S, Shatnyeva O, Shekari F, Shelke GV, Shetty AK, Shiba K, Siljander PR, Silva AM, Skowronek A, Snyder OL, 2nd, Soares RP, Sodar BW, Soekmadji C, Sotillo J, Stahl PD, Stoorvogel W, Stott SL, Strasser EF, Swift S, Tahara H, Tewari M, Timms K, Tiwari S, Tixeira R, Tkach M, Toh WS, Tomasini R, Torrecilhas AC, Tosar JP, Toxavidis V, Urbanelli L, Vader P, van Balkom BW, van der Grein SG, Van Deun J, van Herwijnen MJ, Van Keuren-Jensen K, van Niel G, van Royen ME, van Wijnen AJ, Vasconcelos MH, Vechetti IJ, Jr., Veit TD, Vella LJ, Velot E, Verweij FJ, Vestad B, Vinas JL, Visnovitz T, Vukman KV, Wahlgren J, Watson DC, Wauben MH, Weaver A, Webber JP, Weber V, Wehman AM, Weiss DJ, Welsh JA, Wendt S, Wheelock AM, Wiener Z, Witte L, Wolfram J, Xagorari A, Xander P, Xu J, Yan X, Yanez-Mo M, Yin H, Yuana Y, Zappulli V, Zarubova J, Zekas V, Zhang JY, Zhao Z, Zheng L, Zheutlin AR, Zickler AM, Zimmermann P, Zivkovic AM, Zocco D, and Zuba-Surma EK. 2018. Minimal information for studies of extracellular vesicles 2018 (MISEV2018): a position statement

of the International Society for Extracellular Vesicles and update of the MISEV2014 guidelines. *J Extracell Vesicles* 7:1535750. 10.1080/20013078.2018.1535750

Van der Hauwaert C, Savary G, Gnemmi V, Glowacki F, Pottier N, Bouillez A, Maboudou P, Zini L, Leroy X, Cauffiez C, Perrais M, and Aubert S. 2013. Isolation and characterization of a primary proximal tubular epithelial cell model from human kidney by CD10/CD13 double labeling. *PLoS One* 8:e66750. 10.1371/journal.pone.0066750

Wood CR, and Rosenbaum JL. 2015. Ciliary ectosomes: transmissions from the cell's antenna. *Trends Cell Biol* 25:276-285. 10.1016/j.tcb.2014.12.008

Xiong Z, Cavaretta J, Qu L, Stolz DB, Triulzi D, and Lee JS. 2011. Red blood cell microparticles show altered inflammatory chemokine binding and release ligand upon interaction with platelets. *Transfusion* 51:610-621.

Yoshioka Y, Kosaka N, Konishi Y, Ohta H, Okamoto H, Sonoda H, Nonaka R, Yamamoto H, Ishii H, Mori M, Furuta K, Nakajima T, Hayashi H, Sugisaki H, Higashimoto H, Kato T, Takeshita F, and Ochiya T. 2014. Ultra-sensitive liquid biopsy of circulating extracellular vesicles using ExoScreen. *Nat Commun* 5:3591. 10.1038/ncomms4591

Zecher D, Cumpelik A, and Schifferli JA. 2014. Erythrocyte-derived microvesicles amplify systemic inflammation by thrombin-dependent activation of complement. *Arterioscler Thromb Vasc Biol* 34:313-320. 10.1161/ATVBAHA.113.302378

Zmigrodzka M, Guzera M, Miskiewicz A, Jagielski D, and Winnicka A. 2016. The biology of extracellular vesicles with focus on platelet microparticles and their role in cancer development and progression. *Tumour Biol* 37:14391-14401. 10.1007/s13277-016-5358-6

Table 1(on next page)

Twenty most abundant proteins identified in plasma m/lEVs

Table 1. Twenty most abundant proteins identified in plasma m/lEVs

Protein name	Uniprot AC	Score	Sequence coverage
Ficolin-3	O75636	8772	68
Hemoglobin subunit alpha	P69905	1735	70
Actin, cytoplasmic 1	P60709	927	69
Hemoglobin subunit beta	P68871	602	79
Actin, gamma-enteric smooth muscle	P63267	500	32
Talin-1	Q9Y490	368	50
Filamin-A	P21333	353	40
Spectrin alpha chain, erythrocytic 1	P02549	321	42
Myosin-9	P35579	317	38
Mannan-binding lectin serine protease 1	P48740	308	35
Band 3 anion transport protein	P02730	277	38
Beta-actin-like protein 2	Q562R1	252	24
Hemoglobin subunit delta	P02042	215	64
Spectrin beta chain, erythrocytic	P11277	183	28
Complement C1q subcomponent subunit C	P02747	170	24
Ankyrin-1	P16157	164	28
CD5 antigen-like	O43866	164	52
Integrin alpha-IIb (CD41)	P08514	129	25
Complement C1q subcomponent subunit B	P02746	122	41
Deaminated glutathione amidase	Q86X76	118	6

Proteins in bold text indicate antigens identified using flow cytometry. This table excluded immunoglobulin-related proteins and albumin.

Table 2(on next page)

Twenty most abundant proteins identified in urinary m/lEVs

Table 2. Twenty most abundant proteins identified in urinary m/lEVs

Protein name	Uniprot AC	Score	Sequence coverage
Actin, cytoplasmic 1	P60709	1618	67
Neprilysin	P08473	1194	50
Uromodulin	P07911	821	44
Solute carrier family 12 member 1	Q13621	720	32
Alpha-enolase	P06733	708	79
Moesin	P26038	548	73
Ezrin	P15311	544	56
Aminopeptidase N	P15144	486	43
Actin, gamma-enteric smooth muscle	P63267	476	28
Pyruvate kinase PKM	P14618	447	64
Voltage-dependent anion-selective channel protein 1	P21796	446	74
Radixin	P35241	364	56
Tyrosine-protein phosphatase non-receptor type 13	Q12923	363	38
Triosephosphate isomerase	P60174	325	80
Multidrug resistance protein 1	P08183	324	38
Guanine nucleotide-binding protein G(I)/G(S)/G(T) subunit beta-2	P62879	316	50
Guanine nucleotide-binding protein G(I)/G(S)/G(T) subunit beta-1	P62873	306	53
V-type proton ATPase catalytic subunit A	P38606	298	57
Superoxide dismutase [Cu-Zn]	P00441	285	91
Epidermal growth factor receptor kinase substrate 8-like protein 2	Q9H6S3	277	43

Proteins in bold text indicate antigens identified using flow cytometry

Figure 1

Isolation of m/lEVs from plasma and urine using differential centrifugation

(A and B) Workflow of plasma (A) and urine (B) m/lEV isolation and sample preparation for flow cytometry analysis. (C–H) Isolated m/lEVs from plasma (C–E) and urine (F–H) were visualized by transmission electron microscopy. Arrow indicates representative m/lEVs (C and F). Microscopy was used to identify EV-like particles based on the size (100–400 nm) and shape (round) of the vesicles. The scale bar is shown.

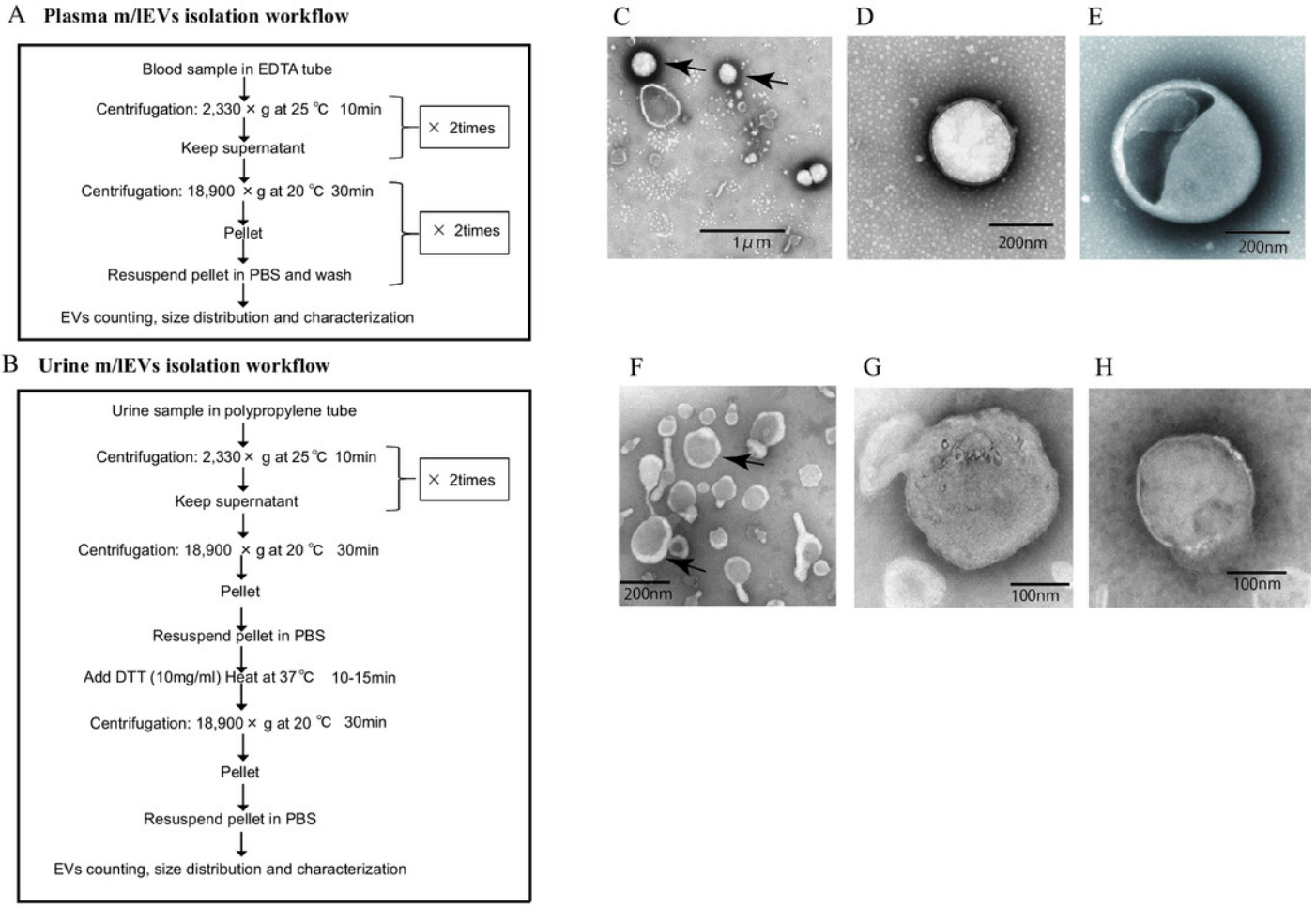

Figure 2

Flow cytometric analysis of plasma and urine m/lEVs

(A and B) Analysis of plasma m/lEVs by flow cytometry. Forward and side scatter (SSC) were measured for plasma m/lEVs (A). The SSC distribution of plasma m/lEVs is shown as a histogram (indigo blue) compared with standard polystyrene beads (black histogram) (B). (C and D) Analysis of urine m/lEVs by flow cytometry. Forward and side scatter (SSC) were measured for urine m/lEVs (C). The SSC distribution of urinary m/lEVs is shown as a histogram (orange) compared with standard polystyrene beads (black histogram) (D).

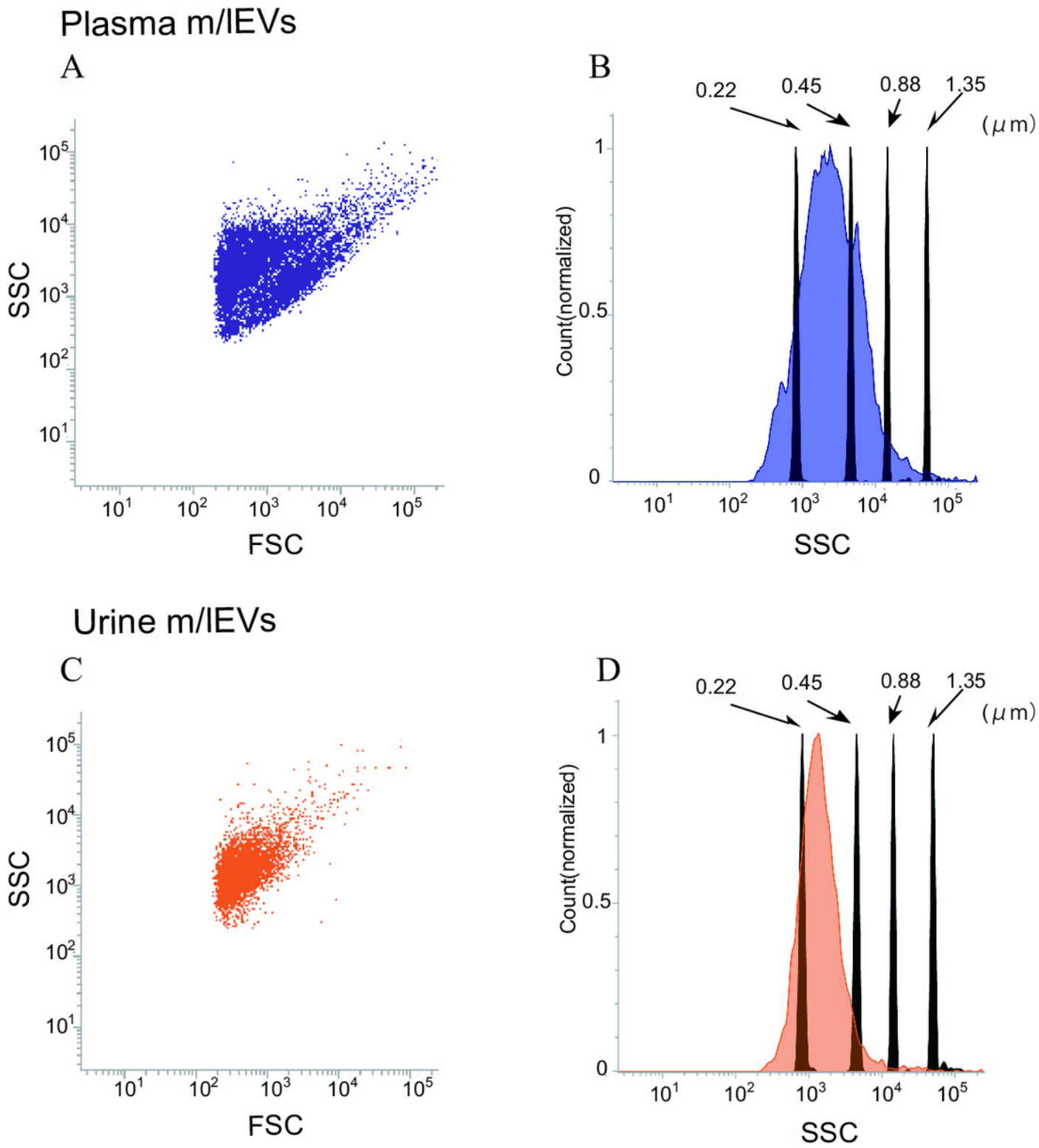
Plasma m/lEVs
A
B
SSC
FSC
Count(normalized)
0.22
0.45
0.88
1.35
(μm)
Urine m/lEVs
C
D

Figure 3

Shotgun proteomic analysis of plasma and urine m/lEVs

A. Protein extracts of m/lEVs isolated from plasma and urine were analyzed by LC-MS/MS. A total of 593 and 1793 proteins from plasma and urine, respectively, were detected. Detailed lists of proteins are shown in S1 Table and S2 Table. B. GO (gene ontology) cellular components are shown for m/lEVs isolated from plasma and urine using the DAVID program. Among the detected proteins, the gene list used for DAVID analysis included 588 proteins (plasma) and 1786 proteins (urine). The vertical axis shows the percentage of proteins from the full gene list categorized into each GO term. For example, for extracellular exosomes (plasma), the categorized count was 301 of 588 proteins. (C and D) Top 20 clusters from the Metascape pathway (http://metascape.org/) enrichment analysis for m/lEVs in plasma (C) and urine (D). Lengths of bars represent log10 (P values) based on the best-scoring term within each cluster. Among all detected proteins, 535 (plasma) and 1767 (urine) genes were recognized as unique for enrichment analysis. For each gene list, pathway and process enrichment analysis was carried out using the following ontology sources: KEGG Pathway, GO Biological Processes, Reactome Gene Sets, Canonical Pathways and CORUM.

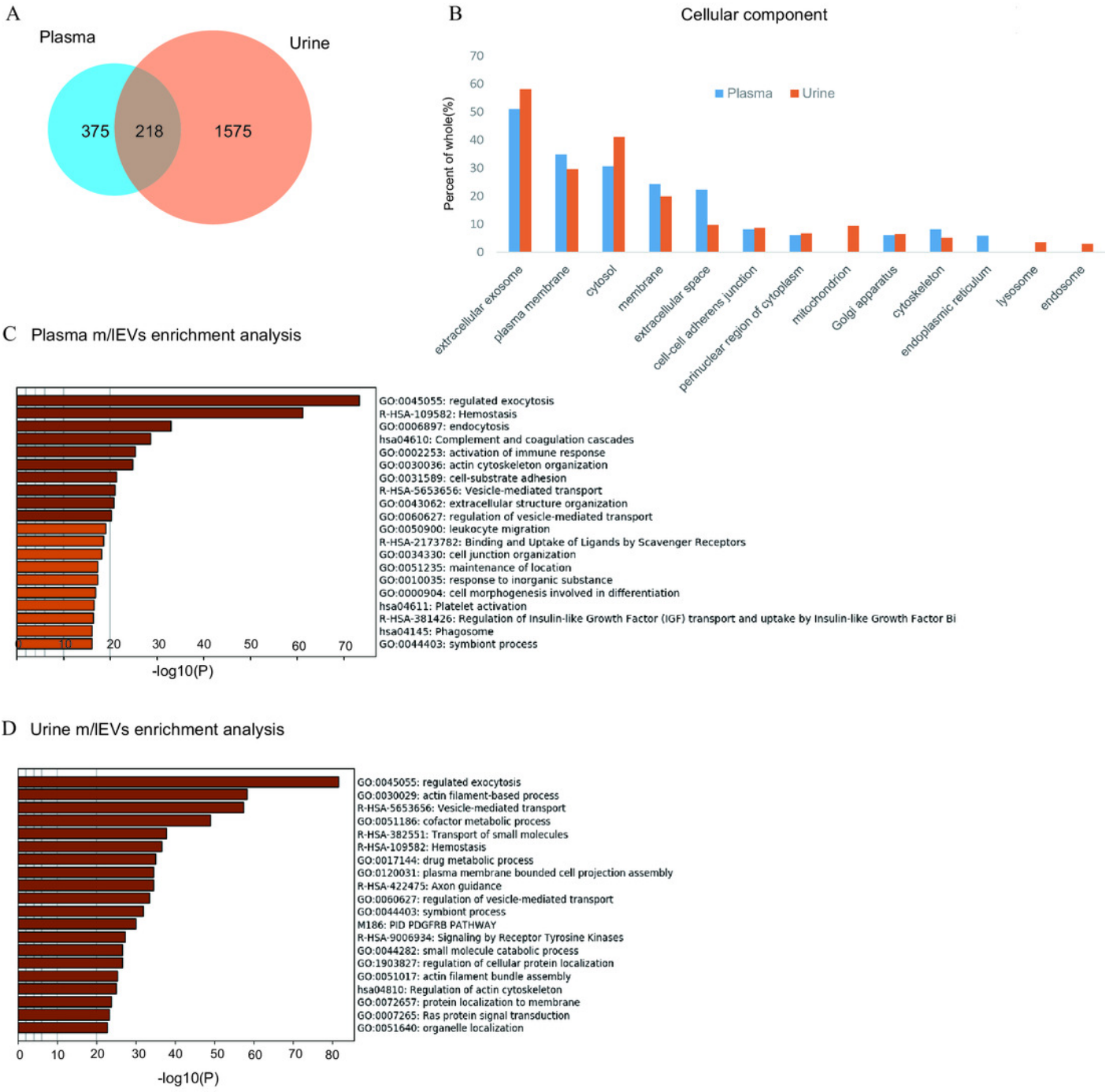
A
Plasma
Urine
375
218
1575
B
Cellular component
Plasma
Urine
Percent of whole(%)
0
10
20
30
40
50
60
70
extracellular exosome
plasma membrane
cytosol
membrane
extracellular space
cell-cell adherens junction
perinuclear region of cytoplasm
mitochondrion
Golgi apparatus
cytoskeleton
endoplasmic reticulum
lysosome
endosome
C Plasma m/lEVs enrichment analysis
GO:0045055: regulated exocytosis
R-HSA-109582: Hemostasis
GO:0006897: endocytosis
hsa04610: Complement and coagulation cascades
GO:0002253: activation of immune response
GO:0030036: actin cytoskeleton organization
GO:0031589: cell-substrate adhesion
R-HSA-5653656: Vesicle-mediated transport
GO:0043062: extracellular structure organization
GO:0060627: regulation of vesicle-mediated transport
GO:0050900: leukocyte migration
R-HSA-2173782: Binding and Uptake of Ligands by Scavenger Receptors
GO:0034330: cell junction organization
GO:0051235: maintenance of location
GO:0010035: response to inorganic substance
GO:0000904: cell morphogenesis involved in differentiation
hsa04611: Platelet activation
R-HSA-381426: Regulation of Insulin-like Growth Factor (IGF) transport and uptake by Insulin-like Growth Factor Bi
hsa04145: Phagosome
GO:0044403: symbiont process
0
10
20
30
40
50
60
70
-log10(P)
D Urine m/lEVs enrichment analysis
GO:0045055: regulated exocytosis
GO:0030029: actin filament-based process
R-HSA-5653656: Vesicle-mediated transport
GO:0051186: cofactor metabolic process
R-HSA-382551: Transport of small molecules
R-HSA-109582: Hemostasis
GO:0017144: drug metabolic process
GO:0120031: plasma membrane bounded cell projection assembly
R-HSA-422475: Axon guidance
GO:0060627: regulation of vesicle-mediated transport
GO:0044403: symbiont process
M186: PID PDGFRB PATHWAY
R-HSA-9006934: Signaling by Receptor Tyrosine Kinases
GO:0044282: small molecule catabolic process
GO:1903827: regulation of cellular protein localization
GO:0051017: actin filament bundle assembly
hsa04810: Regulation of actin cytoskeleton
GO:0072657: protein localization to membrane
GO:0007265: Ras protein signal transduction
GO:0051640: organelle localization
0
10
20
30
40
50
60
70
80
-log10(P)

Figure 4

Characterization of plasma m/lEVs by flow cytometry

A. Two specific surface antigens were used to characterize the m/lEVs from each source by flow cytometry. m/lEVs were characterized by comparison with five types of blood cells using surface antigens and Annexin V staining. (B and C). Representative dot plots (SSC vs. Annexin V). Each plot was classified by staining for surface antigens and Annexin V (C) and an overall plot summarizing the data (B) is shown. D. Quantification of each m/lEV by flow cytometry analysis (n=10 for human healthy plasma, % of total events). E. Comparison of Annexin V staining for erythrocyte-, platelet-, macrophage-, T and B cell-, and endothelial cell-derived m/lEVs from ten healthy plasma samples. Comparisons were performed using the Wilcoxon signed-rank test (* $p< 0.05$, ** $p < 0.01$; a value of $p < 0.05$ was considered to indicate statistical significance).

A Plasma m/IEVs characterized by multi CD antigen

	Annexin5	CD59 · Protectin · MIRL	CD235a · Glycophorin A	CD41 · Integrin αIIb	CD61 · Integrin β3	CD15 · Lewis x · SSEA-1	CD45 · Leukocyte Common Antigen	CD5 · Leu-1	CD105 · Endoglin	CD146 · Muc 18
Erythrocyte derived	+	+	+				-			
	-	+	+				-			
Platelet derived	+			+	+		-	-		
	-			+	+		-	-		
Macrophage/Monocyte/Granulocyte derived	+		-			+	+			
	-		-			+	+			
T and B cell derived	+		-				+	+		
	-		-				+	+		
Endothelial Cell derived	+								+	+
	-								+	+

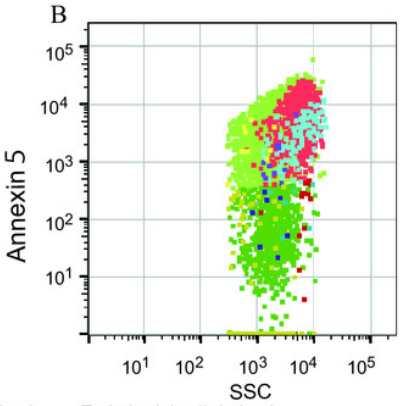

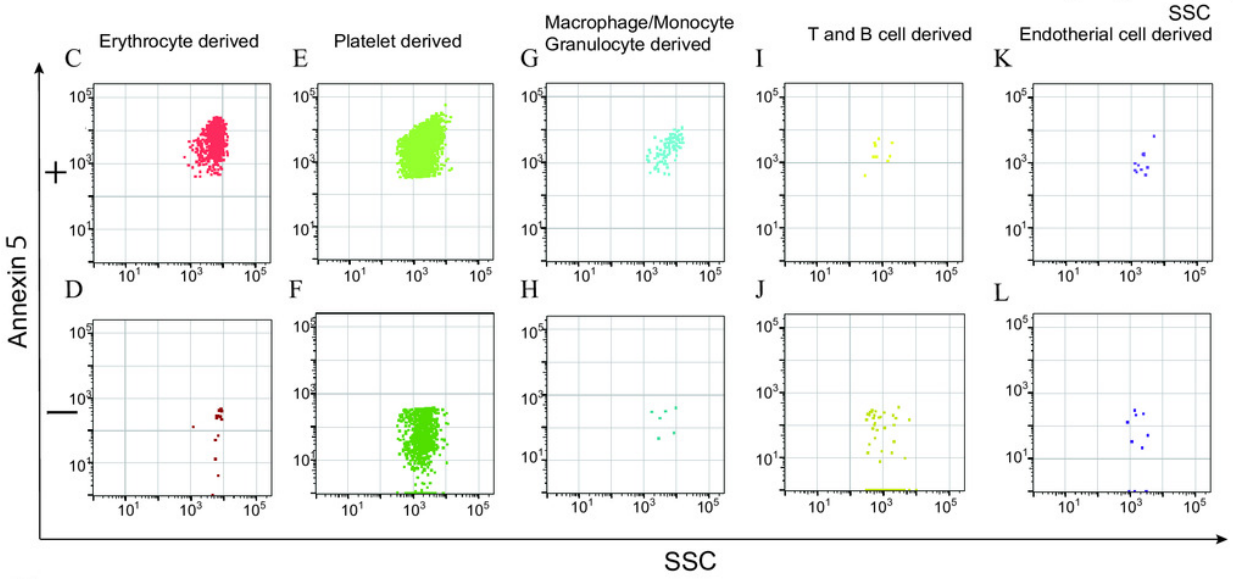

M

Characterized m/IEVs ratio in 10 healthy plasma

	(N=10)	Annexin5	Average(%)	SD	range (%)
Erythrocyte derived		+	10%	4.2%	2.8-16
		-	0.16%	0.25%	0-0.84
Platelet derived		+	19%	8.2%	4.6-30
		-	16%	10%	2.6-32
Macrophage/Monocyte/Granulocyte derived		+	0.43%	0.49%	0.02-1.3
		-	0.07%	0.10%	0-0.31
T and B cell derived		+	0.19%	0.24%	0.01-0.77
		-	0.50%	0.40%	0.05-1.4
Endothelial Cell derived		+	0.08%	0.05%	0.02-0.2
		-	0.03%	0.03%	0.01-0.09

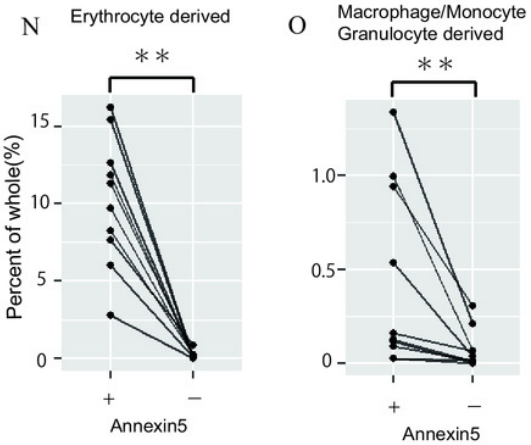

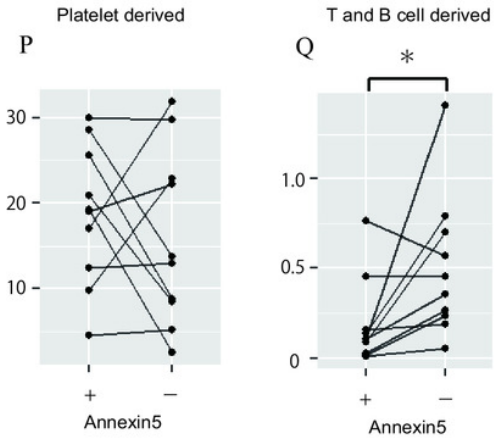

Figure 5

Characterization of urinary m/lEVs by flow cytometry and CD26 enzymatic activity

A. Two kinds of m/lEVs in urine were characterized by using surface antigen and Annexin V staining. B. Representative dot plots in the observation area (SSC vs Annexin V). Each plot was classified according to staining for multiple peptidases [CD10 (neprilysin), CD13 (alanine aminopeptidase), and CD26 (DPP4)] and CD277 (MUC-1). Events were further classified as Annexin V positive or negative. C. Quantification of m/lEVs by flow cytometry analyses (n=10 for male human healthy urine, % of total events). D. Comparison of Annexin V staining for MUC1-positive and multiple peptidase-positive m/lEVs in the urine of ten healthy male human samples. Comparisons were performed using the Wilcoxon signed-rank test (* $P < 0.05$, ** $P < 0.01$; a value of $p < 0.05$ was considered to indicate statistical significance). E. DPP4 enzymatic activity was assessed for urinary m/lEVs. The workflow for fractionating m/lEVs by centrifugation is shown. F. Quantification of DPP4 activity in plasma and urine fractions (n=6 for human healthy plasma and male urine, % of whole). The percentage of enzyme activity measured for each fraction compared with whole activity is shown.

A Urine m/IEVs characterized by multi CD antigen

	Annexin5	CD10 ・neutral endopeptidase ・Neprilysin	CD13 ・Amino peptidase N	CD26 ・Dipeptidyl Peptidase-4 (DPPIV)	CD227 ・Mucin 1 (MUC1)
Multiple peptidase positive	+	+	+	+	-
	-	+	+	+	-
MUC1 positive	+		-		+
	-		-		+

G Characterized m/IEVs ratio in 10 healthy male urine

(N=10)	Annexin5	Average(%)	SD	range (%)
Multiple peptidase (CD10,CD13,CD26)	+	10%	9.0%	2.2-28
positive	-	38%	17%	11-68
MUC1 positive	+	5.2%	3.4%	2.0-12
	-	3.2%	2.6%	0.82-9.4

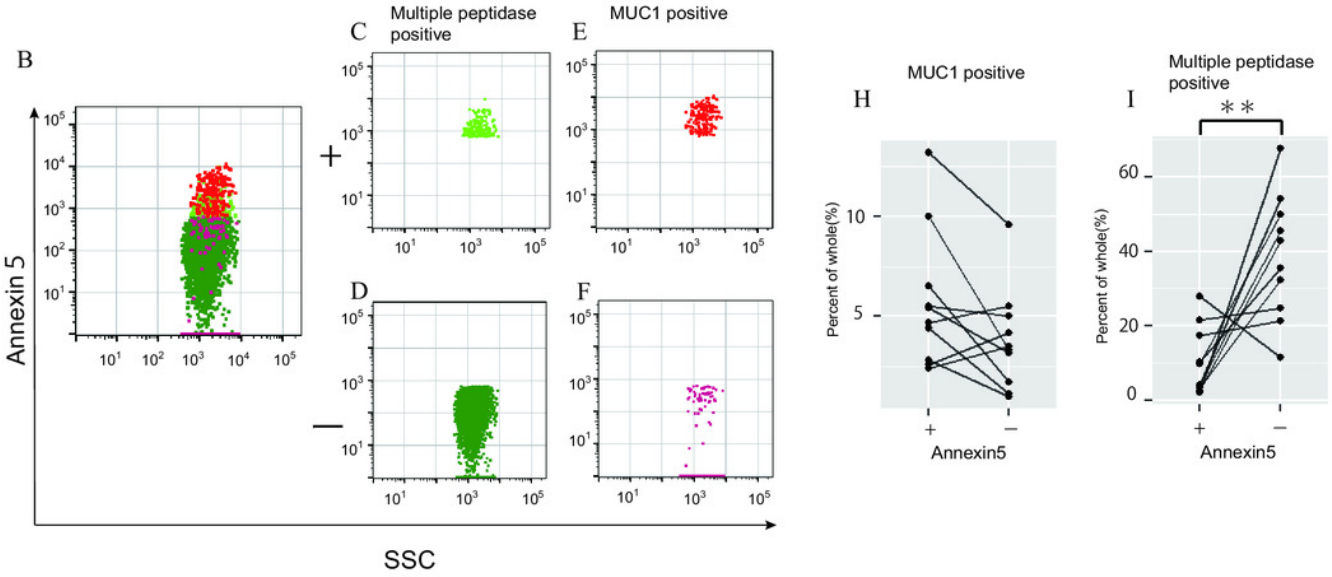

J DPP4(CD26) activity of plasma and urine m/IEVs